

# MgB<sub>2</sub>: superconductivity and pressure effects

V. A. Ivanov, J. J. Betouras, and F. M. Peeters  
Departement Natuurkunde, Universiteit Antwerpen (UIA),  
Universiteitsplein 1, B-2610 Antwerpen, Belgium

## Abstract

The Ginzburg-Landau theory is presented for a two-band superconductor with emphasis on MgB<sub>2</sub>. Experiments are proposed which lead to identification of the possible scenarios: whether both  $\sigma$ - and  $\pi$ -bands superconduct or  $\sigma$ -alone. According to the second scenario a microscopic theory of superconducting MgB<sub>2</sub> is proposed based on the strongly interacting  $\sigma$ -electrons and non-correlated  $\pi$ -electrons of boron ions. The kinematic and Coulomb interactions of  $\sigma$ -electrons provide the superconducting state with an anisotropic gap of  $s^*$ -wave symmetry. The critical temperature  $T_c$  has a non-monotonic dependence on the distance  $r$  between the centers of gravity of  $\sigma$ - and  $\pi$ -bands. The position of MgB<sub>2</sub> on a bell-shaped curve  $T_c(r)$  is identified in the overdoped region. The derived superconducting density of electronic states is in agreement with available experimental and theoretical data. It is argued that the effects of pressure are crucial to identify the microscopic origin of superconductivity in MgB<sub>2</sub>. Possibilities for  $T_c$  increase are discussed.

The discovery of superconductivity in MgB<sub>2</sub> [1] poses many interesting and fundamental questions regarding the nature of the superconducting state as well as the possibility of multi-band superconductivity. The crystal belongs to the space group  $P6/mmm$  or  $AlB_2$ -structure where borons are packed in honeycomb layers alternating with hexagonal layers of magnesium ions. The ions Mg<sup>2+</sup> are positioned above the centers of hexagons formed by boron sites and donate their electrons to the boron planes. The electronic structure is organized by the narrow energy bands with near two-fold degenerate  $\sigma$ -electrons and the wide-band  $\pi$ -electrons. Without any of the lattice strain, the  $\sigma$  dispersion relations are slightly splitted due to the two boron atoms per unit cell. The corresponding portions of the Fermi surface consist of coaxial cylinders along the  $\Gamma$  - A symmetry direction of the Brillouin zone (BZ), whereas the  $\pi$ - bands are strongly dispersive. In the following sections we present a Ginzburg-Landau (GL) analysis of the two-band superconductor with emphasis on MgB<sub>2</sub>, we apply it in pressure experiments which potentially distinguish the different superconducting bands [2], then we provide a microscopic model.

# 1 Ginzburg-Landau analysis and pressure effects

We distinguish different possibilities:

*Case I: Both  $\sigma$  and  $\pi$  bands superconduct.* The GL free energy functional for MgB<sub>2</sub> in this case can be written as :

$$F = \int d^3r \left\{ \frac{1}{2m_\sigma} |\vec{\Pi}\psi_\sigma|^2 + \alpha_\sigma |\psi_\sigma|^2 + \beta_\sigma |\psi_\sigma|^4 + \frac{1}{2m_\pi} |\vec{\Pi}\psi_\pi|^2 + \alpha_\pi |\psi_\pi|^2 + \beta_\pi |\psi_\pi|^4 \right. \\ \left. + r(\psi_\sigma^* \psi_\pi + \psi_\sigma \psi_\pi^*) + \beta(|\psi_\sigma|^2 |\psi_\pi|^2) + \frac{(\vec{\nabla} \times \vec{A})^2}{8\pi} \right\}, \quad (1)$$

where  $\vec{\Pi} = -i\hbar\vec{\nabla} - 2e/c\vec{A}$  and  $\vec{A}$  is the vector potential,  $\alpha_{\sigma,\pi} = \alpha_{\sigma,\pi}^0(T - T_{c\sigma,\pi}^0)$ .

(i) If  $r = 0$  then Eq. 1 is the free energy for two bands without pairing transfer (Josephson coupling) between them. The quartic term which mixes the two order parameters reflects the fact that although the two bands are different, there is a constraint coming from the common chemical potential which connects them in equilibrium. It is also the realization and a measure of the strength of the interband interaction of quasiparticles and it affects the critical temperatures. The absence of a bilinear in the two order parameters term facilitates the observation of the Leggett's mode in the Josephson tunneling between a two-band superconductor and an ordinary superconductor [3]. The onset of the superconducting state in one band does not imply the onset in the other. To investigate this possibility in MgB<sub>2</sub> an experiment which checks the splitting of the transitions due to the lattice deformation by the strain fields can be decisive. In the MgB<sub>2</sub> the compression due to pressure is anisotropic[4, 5, 6]. According to Ref. [4] the compressibility along the  $c$ -axis is almost twice larger than that of the plane compressibility. Therefore application of uniaxial pressure on single crystals will affect differently the two gaps and the result will be a splitting of the critical temperatures, even if at ambient pressure they appear to be the same. This can be measured through a specific heat experiment under pressure. Following Ozaki's formulation [7, 8], we add to the GL functional Eq.(1) the term which couples the order parameters, in second order, with the strain tensor  $\epsilon$  to first order.

$$F_{strain} = -C_1(\Gamma_1)[\delta(\epsilon_{xx} + \epsilon_{yy}) + \epsilon_{zz}]|\psi_\sigma|^2 - C_2(\Gamma_1)(\epsilon_{xx} + \epsilon_{yy} + \epsilon_{zz})|\psi_\pi|^2, \quad (2)$$

where  $C_{1,2}(\Gamma_1)$  are coupling constants,  $\delta$  is given in terms of the elastic constants of the material  $\delta = (c_{11} + c_{12} - c_{13})/(c_{13} - c_{33})$ . The effect of the pressure on these two order parameters, each one belonging to an one-dimensional representation is to shift the critical temperatures. The new critical temperatures can be found, by solving the coupled equations for  $|\psi_{\sigma,\pi}|^2$  and then setting the coefficients of  $|\psi_{\sigma,\pi}|^2$  to zero. The result is :  $T_{c\sigma,\pi} = T_{c\sigma,\pi}^0 - \eta_{\sigma,\pi} \times p$ , where for uniaxial pressure  $\eta_\pi > \eta_\sigma > 0$ . In order to detect the splitting, the pressure must be above a certain value  $p_{min}$  which depends on the resolution of the experiment, so that the difference in the two critical temperatures  $\Delta T_c = |T_{c\sigma}^0 - T_{c\pi}^0 + \eta_\sigma - \eta_\pi|p_{min}$  is experimentally detectable.

(ii) If  $r \neq 0$  then the pair transferring term is present and it means that the onset of superconductivity in one band implies automatically the appearance of superconductivity in the other. There is a single observed  $T_c$  with a different pressure dependence. Analyzing the equations which result from the minimization of the GL free energy we get in the regime  $T_{c\sigma}^0 > T > T_{c\pi}^0$  :

$$\frac{\alpha_\pi \alpha_\sigma}{2\beta_\sigma} = -r^2 \quad (3)$$

This gives the pressure dependence of the  $T_c$ :

$$T_c(p) = \frac{1}{2} [T_{c\sigma}^0 + T_{c\pi}^0 - (\eta_\pi + \eta_\sigma)p] + \frac{1}{2} [(T_{c\sigma}^0 - T_{c\pi}^0 - (\eta_\pi - \eta_\sigma)p)^2 - a^2]^{1/2} \quad (4)$$

and  $a^2 = 8\beta_\sigma r^2 / (\alpha_\pi^0 \alpha_\sigma^0)$ . Deviations from a straight line at moderate values of pressure can be attributed to the two bands.

*Case II: Only the  $\sigma$ - bands superconduct.* In this case there is one order parameter initially and the GL free energy functional is the usual one. The dominant physical situation is an important change in the electronic properties of the material under pressure, because the band ( $\sigma_2$ ) which is below the Fermi level at ambient pressure [9] can, partially, overcome the barrier and get above the Fermi level at a certain value of pressure (crossover pressure), restoring the degeneracy of the two  $\sigma$  bands at point  $\Gamma$ . Then there will be a crossover from a superconducting state  $\psi_1$  to a state  $\psi_1 + \psi_2$ . To understand this effect we need to write the GL free energy taking into account the second order parameter of the same symmetry as well as the hexagonal symmetry of the boron layers. The irreducible representation of the  $D_{6h}$  group are four one-dimensional ones (three of them have line nodes) and two two-dimensional ones [8]. There are experimental data compatible with  $s$ -wave or an anisotropic  $s^*$ -wave order parameter. and a penetration depth experiment [10] which suggests nodes or anisotropic  $s^*$ -wave. Therefore we consider the gap to be a function of  $k_x$  and  $k_y$  with a smooth modulation in the  $k_z$  direction as in Ref. [15]. As a consequence the most promising candidates for the initial order parameter are the basis functions of the  $\Gamma_1$  representation of the  $D_{6h}$  group. To construct the functional of the free energy for two order parameters, we need to take into account the decomposition of the terms containing the derivatives  $\vec{\Pi}$ , which belong to the  $\Gamma_5$  representation. Then the decomposition

$$\Gamma_5^* \otimes \Gamma_1^* \otimes \Gamma_5 \otimes \Gamma_1 = \Gamma_1 + \Gamma_2, \quad (5)$$

contains the  $\Gamma_1$  representation once and suggests that there is precisely one term quadratic in  $\Pi_{x,y}$  which mixes the two order parameters (to first order each). There is also a quadratic term which mixes the two components, according to the trivial decomposition  $\Gamma_1 \otimes \Gamma_1$  and a quartic term as well. Taking into accounts all the usual

terms, we obtain the following expression for the free energy:

$$F = \int d^3r \left\{ \frac{1}{2m_1} |\vec{\Pi}\psi_1|^2 + \alpha_1 |\psi_1|^2 + \beta_1 |\psi_1|^4 + \frac{1}{2m_2} |\vec{\Pi}\psi_2|^2 + \alpha_2 |\psi_2|^2 + \beta_2 |\psi_2|^4 + \right. \\ \left. \gamma_1 (\psi_1^* \psi_2 + c.c.) + \gamma_2 (\Pi_x \psi_1 \Pi_x^* \psi_2^* + \Pi_y \psi_1 \Pi_y^* \psi_2^* + c.c.) + \beta_3 (|\psi_1|^2 |\psi_2|^2) + \frac{(\vec{\nabla} \times \vec{A})^2}{8\pi} \right\}. \quad (6)$$

We have used the fact that the  $\gamma_1$ -term favors the coupling of linear combination of the two order parameters with phase difference 0 or  $\pi$  between them [11], therefore a term  $\psi_1^{2*} \psi_2^2 + c.c.$  is incorporated into the  $\beta_3$ -term of the free energy. The resemblance between Eq.(1) and Eq.(7) is apparent; in the first case the mixing terms are a consequence of the interactions between the two bands, in the second case it is due to the modification of the existing gap in the electronic spectrum.

With the present approach we are in the position to describe the crossover and to consider the possibility of different effective masses and parameters (the inclusion of the effect at  $p_c$ ). The effect of pressure can be taken into account as usual [12] with the modification due to the particular physical situation by writing  $\alpha_2 = \alpha_2^0 (T - T_c(p)) \Theta(p - p_c)$ ,  $\gamma_1 = \gamma_1^0 (p - 1) \Theta(p - p_c)$ . The additional term which couples the order parameter with the strain tensor  $\epsilon$ , in the regime where  $p > p_c$  is :

$$F_{strain} = -C(\Gamma_1) [(1 + \delta)(\epsilon_{xx} + \epsilon_{yy}) + 2\epsilon_{zz}] \times |\psi_1 + \psi_2|^2.$$

The coupling to strain affects both order parameters in the same way.

The approximate value of the crossover pressure can be estimated as follows. The energy difference between the two subbands is approximated by  $(1 - n_\sigma)^2 \Delta$ , where the fraction of superconducting electrons is  $1 - n_\sigma \sim 0.03$ , *i.e.* the carrier density per boron atom in  $MgB_2$ . The approximate value of the crossover pressure  $p_c$  which suppresses the deformation potential  $\Delta$  can be estimated by the expression  $p_c \Omega \sim (1 - n_\sigma) \sqrt{\Delta}$  where  $\Omega = 30 \text{\AA}^3$  is a unit cell volume of  $MgB_2$  and  $\Delta = 0.04 eV^2$  is the deformation potential for a boron displacement  $u \sim 0.03 \text{\AA}$  [13]. Using these parameters, we get a crossover pressure of  $p_c \sim 30 GPa$ . This estimation shows, that an applied pressure at a realistic value influences drastically the electronic structure, producing the degeneracy of two bands which are initially splitted. Superconductivity in the second band will occur at lower values of the estimated  $p_c$ . The requested band overlapping around the Fermi energy will also occur at lower values due to the corrugation of the Fermi surfaces and the already existing strains in the material and the anisotropic compressibility. These considerations make the above estimation an upper limit of  $p_c$ . The degree to which shear stresses of the sample and the surrounding fluid under pressure affect the data of pressure measurements is still under investigation [14]. The physics of this crossover is similar in spirit to an electronic topological transition of 5/2 kind [16]. In Fig.1 in a model calculation, we illustrate the expected behavior of  $T_c$  and the form of the order parameter as a function of pressure at fixed temperature and schematically the kink at  $p_c$  of  $T_c$ .

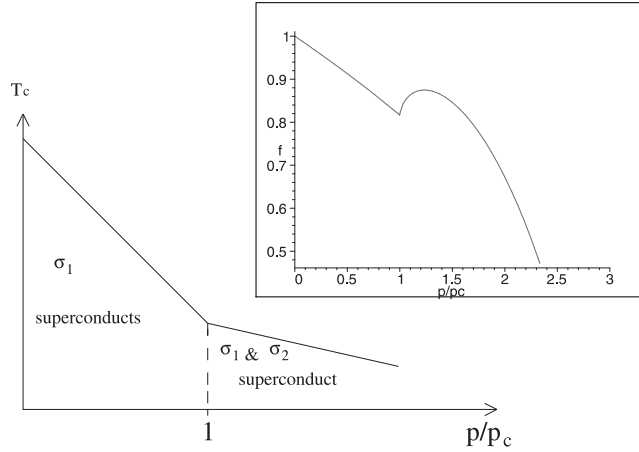


Figure 1: The form of  $T_c$  as a function of pressure for case II,  $p_c$  is the crossover pressure where the second band becomes superconducting as well. Frame: The order parameter  $f = |\psi_1(p) + \psi_2(p)|/|\psi_1(0)|$  at  $T = 0.7T_{c1}$ . The chosen parameters are:  $\alpha_1 = 2(T/T_{c1} - 1 - 0.1p/p_c)$ ,  $\alpha_2 = (T/T_{c1} - 0.8 - 0.1p/p_c)$ ,  $\beta_1 = \beta_2 = 1$ ,  $\beta_3 = \Theta(p/p_c - 1)$ ,  $\gamma_1 = 0.4(p/p_c - 1)\Theta(p/p_c - 1)$ .

The anomaly close to  $p_c$  can be detected directly in a penetration depth experiment under pressure.

The picture we provide for the second case is complimentary to the first. Both cases may be realized since the effects can be detected at different values of pressures. In case I, the value of pressure necessary to see the effects is limited either by the experimental resolution or by the validity of the Eq. 4 at low pressure. The specific symmetry of the order parameters is only used to produce the additional terms due to strain. In case II there is a larger predicted value for the crossover pressure and there are more specific assumptions regarding the symmetry of the order parameter. Early pressure experiments [17] demonstrated the overall decrease of  $T_c$  with pressure which was attributed to the loss of holes. In two of the samples there is a linear dependence of  $T_c$  on pressure and in two others a weak quadratic dependence. We stress that the samples are polycrystalline and the experiment is effectively under hydrostatic pressure. Also the degree of nonstoichiometry was not known. The almost linear dependence for a wide range of pressures, makes the GL functional as presented, valid for the  $\text{MgB}_2$ . Experiments on single crystals will be able to verify the effects which are described. We do not attempt at the moment any fitting of experimental data because there is no experimental consensus on the different values of key parameters of the theory (e.g. there is a wide range of published data on the value of  $dT_c/dp$  [14]).

## 2 Microscopic model

The presented microscopic model of superconductivity in MgB<sub>2</sub>, is based on the correlated  $\sigma$ - and the non-correlated  $\pi$ -band. The negatively charged boron layers and the positively charged magnesium layers provide a lowering of the  $\pi$ -band with respect to the  $\sigma$ -band which was also noticed first in band calculations [18, 19]. In this microscopic treatment the  $\sigma$ -bands are treated as degenerate. The quasi-2D  $\sigma$ -electrons are more localized than the 3D  $\pi$ -electrons. This leads to an enhancement of the on-site electron correlations in the system of degenerated  $\sigma$ -electrons. They are taken to be infinite, while the intersite Coulomb interactions and electron-phonon interactions simply shift the on-site electron energies. After carrying out a fermion mapping to  $X$ -operators the Hamiltonian becomes:

$$\begin{aligned}
 H = & \sum_{p,s} t^{(\sigma)}(p) X^{so}(p) X^{os}(p) + V \sum_{\langle i,j \rangle} n_{\sigma}(i) n_{\sigma}(j) - r \sum_i n_{\pi}(i) + \\
 & + \sum_{p,s} \varepsilon_0^{(\pi)}(p) [\pi_s^+(p) \pi_s(p) + H.c.] - \mu \sum_i [n_{\sigma}(i) + n_{\pi}(i)]. \quad (7)
 \end{aligned}$$

Here, the  $X$ -operators describe the on-site transitions of correlated  $\sigma$ -electrons between the one-particle ground states (with spin projection  $s = \pm$ ) and the empty polar electronic states (0) of the boron sites and  $\mu$  is the chemical potential. The wide  $\pi$ -band is shifted with respect to the  $\sigma$ -band by an energy  $r$ , comprising the mean-field  $\pi$ -electron interactions and the electron-phonon interactions. We included in Eq. (7) also the nearest neighbour Coulomb repulsion  $V$  of  $\sigma$ -electrons, which is essential for the low density of hole-carriers in MgB<sub>2</sub>. The mutual hopping between  $\sigma$ - and  $\pi$ -electrons is assumed to be negligible due to the characteristic space symmetry of the orbitals involved. A schematic view of the model is presented in Fig. 2.

The diagonal  $X$ -operators ( $X^{\cdot} \equiv X^{\cdot\cdot}$ ) satisfy the completeness relation,  $X^0 + 4X^s = 1$ , and their thermodynamic averages ( $\langle X^0 \rangle$ ,  $\langle X^s \rangle$ ) are the Boltzmann populations of the energy levels of the unperturbed on-site Hamiltonian in (7). Due to the orbital and spin degeneracy the  $\sigma$ -electrons occupy their one-particle ground state with density  $n_{\sigma} = 4 \langle X^s \rangle$  per boron site. The correlation factor for the degenerated  $\sigma$ -electrons is  $f = \langle X^0 + X^s \rangle = 1 - 3 \langle X^s \rangle = 1 - \frac{3}{4} n_{\sigma}$ . It plays an important role in all numerics starting from their unperturbed (zeroth order) Green's function,  $D_{\sigma}^{(0)}(\omega) = f / (-i\omega_n - \mu)$ , whereas for  $\pi$ -electrons  $D_{\pi}^{(0)}(\omega) = 1 / (-i\omega_n - \mu - r)$ . Note that for the conventional Hubbard model the correlation factor in the paramagnetic phase is  $1 - n/2$  (see [23] and Refs. therein).

The energy dispersion of both bands,  $\xi(p) = ft(p) - \mu$  and  $\varepsilon(p) = \varepsilon_0(p) - r - \mu$ , are governed by the zeros of the inverse Green's function  $D^{-1}(\omega, p) = \text{diag} \{ D_{\sigma}^{-1}(\omega, p); D_{\pi}^{-1}(\omega, p) \} = \text{diag} \left\{ \frac{-i\omega_n + \xi(p)}{f}; -i\omega_n + \varepsilon(p) \right\}$ , which follows from the Dyson equation  $D^{-1}(\omega, p) = D^{(0)-1}(\omega) + \hat{t}(p)$ , to first order with respect to the

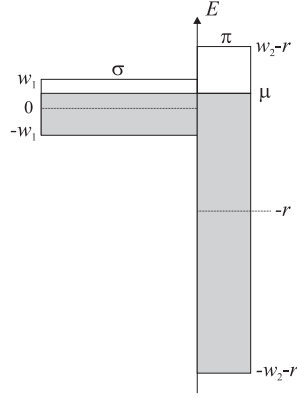


Figure 2: A schematic view of the energy band diagram. The degenerate  $\sigma$ -electrons are represented by a lower correlated band.

tunneling matrix  $\hat{t}(p) = \text{diag}\{t(p); \varepsilon_0(p)\}$ .

The chemical potential  $\mu$  for the  $\text{MgB}_2 = \text{Mg}^{++}\text{B}^-(p^2)_2 = \text{Mg}^{++}\text{B}^-(p^{n_\sigma}p^{n_\pi})_2$ -system (Eq. (1)) obeys the equation for the total electron density per boron site  $n_\sigma + n_\pi = 2$ , with the partial electron densities:

$$n_{\sigma,\pi} = 2T \sum_{n,p} e^{i\omega\delta} D_{\sigma,\pi}(\omega, p) \equiv n_{\sigma,\pi}(r, \mu). \quad (8)$$

The electron densities satisfy the requirements  $0 < n_\sigma < 1$  (due to the correlation factor  $f$ , providing the quarter-fold narrowing of the degenerate  $\sigma$ -band) and  $0 < n_\pi < 2$ . For any energy difference  $r$  between the  $\sigma$ - and  $\pi$ -bands the chemical potential  $\mu$  has to be such that the constraint  $n_\sigma + n_\pi = 2$  is satisfied.

From the system of Eqs. of the constraint and (9), for a flat density of electronic states (DOS hereafter)  $\rho_{\sigma,\pi}(\varepsilon) = (1/2w_{1,2})\theta(w_{1,2}^2 - \varepsilon^2)$  with half-bandwidths  $w_1$  and  $w_2$  for  $\sigma$ - and  $\pi$ -electrons, respectively) we derive the chemical potential of the  $A^{2+}B(p^{n_\sigma}p^{n_\pi})_2$  systems as

$$\mu = \frac{w_2 - 5r}{5w_1 + 4w_2}w_1. \quad (9)$$

The non-correlated  $\pi$ -electrons play the role of a reservoir for the  $\sigma$ -electrons. In the energy dispersion  $\xi(p)$  for the  $\sigma$ -electrons, the correlation factor  $f$  can be expressed also via the parameters  $w_1, w_2$  and  $r$  as  $f = (2w_1 + w_2 + 3r) / (5w_1 + 4w_2)$ .

The anomalous self-energy for the  $\sigma$ -electrons (Fig. 3) is written self-consistently as

$$\overset{\vee}{\Sigma}(p) = T \sum_{n,q} \Gamma_0(p, q) \frac{\overset{\vee}{\Sigma}(q)}{\omega_n^2 + \xi^2(q) + \overset{\vee}{\Sigma}(q)}, \quad (10)$$

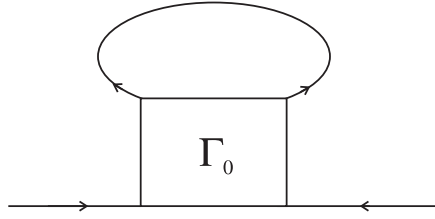


Figure 3: The anomalous self-energy  $\overset{\vee}{\Sigma}(p)$  for  $\sigma$ -electrons. The solid line is an anomalous Green's function.

where the vertex  $\Gamma_0$  is determined by the amplitudes of the kinematic and Coulomb interactions such that  $\Gamma_0(p, q) = -2t_q + V(p - q)$ . We do not include the other kinematic vertices in  $\Gamma_0$  which are essential at a moderate concentration of carriers [23].

In momentum space the Coulomb repulsion between the nearest neighbours (Eq. (7)) reflects the tight-binding symmetry of the boron honeycomb lattice [22]. Near the  $\Gamma - A$  line of the Brillouin zone the Coulomb vertex can be factorized as  $V(p - q) = 2\beta t(p)t(q)$ , where the parameter  $\beta = V/6t^2$  expresses the Coulomb repulsion for the nearest  $\sigma$ -electrons and the energy dispersion is  $t(p) = 3t \left(1 - \frac{p_x^2 + p_y^2}{12}\right)$ . Considering the explicit form of the vertex  $\Gamma_0$  in Eq. (10), and after summation over the Matsubara frequencies  $\omega_n = (2n + 1)\pi T$  one obtains

$$\overset{\vee}{\Sigma}(p) = \sum_q t(q) (1 - \beta t(p)) \overset{\vee}{\Sigma}(q) \frac{\tanh \sqrt{\xi^2(q) + \overset{\vee}{\Sigma}^2(q)}/2T}{\sqrt{\xi^2(q) + \overset{\vee}{\Sigma}^2(q)}}. \quad (11)$$

The search for a solution in the form  $\overset{\vee}{\Sigma}(p) = \Sigma_0 + t(p)\Sigma_1$  converts Eq. (11) for the superconducting critical temperature and the gap to

$$1 = \sum_p t(p) (1 - \beta t(p)) \frac{\tanh \sqrt{\xi^2(p) + \Sigma^2(p)}/2T}{\sqrt{\xi^2(p) + \Sigma^2(p)}}, \quad (12)$$

with the gap function  $\Sigma(p) = [1 - \beta t(p)]\Sigma_0$ .

Setting the gap function in Eq. (12) equal to zero, one can derive analytically  $T_c$  in a logarithmic approximation:

$$\begin{aligned} T_c &= \frac{w_1}{5w_1 + 4w_2} \sqrt{(w_1 + w_2 - r)(w_1 + 4r)} \exp\left(-\frac{1}{\lambda}\right), \\ \lambda &= \frac{(5w_1 + 4w_2)(3 + 5\beta w_1)}{(2w_1 + w_2 + 3r)^3} (w_2 - 5r) \left[ r - \frac{\beta w_1 w_2 - 2w_1 - w_2}{3 + 5\beta w_1} \right]. \end{aligned} \quad (13)$$

Under the prefactor in the square root the restrictions for an energy shift  $r$  guarantee the assumed volume of the correlated  $\sigma$ -band, namely  $n_\sigma \geq 0$  ( $r \leq w_1 + w_2$ ) and

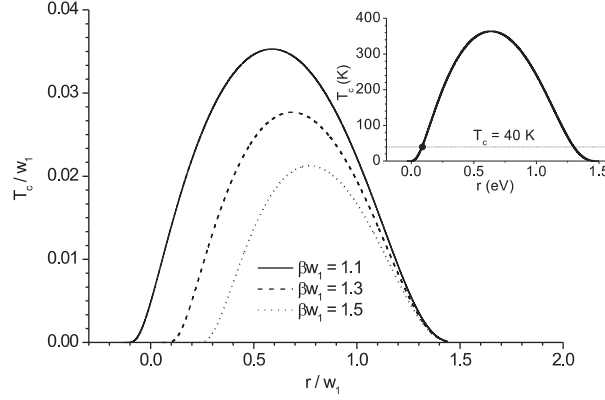


Figure 4: The non-monotonic dependence of  $T_c(r)$  at different magnitudes of the Coulomb repulsion (parameter  $\beta w_1$ ). Here  $w_2/w_1 = 8$ . MgB<sub>2</sub> is marked in the inset with a solid circle positioned at  $r = 0.085$  eV and  $\beta w_1 = 1.2$  for  $w_1 = 1$  eV and  $w_2 = 8$  eV.

$n_\sigma \leq 1$  ( $r \geq -w_1/4 = -t$ ).  $T_c(r)$  is plotted in Fig. 4 for different values of the parameter  $\beta$ , reflecting the suppression of superconductivity with an increase of the Coulomb repulsion. In the MgB<sub>2</sub> case,  $T_c = 40$  K, corresponds to  $r = 0.085$  eV and a dimensionless value  $\beta w_1 = 8 \text{ V}/3w_1$ .

The superconducting gap equation follows from Eq. (12) taken for  $T=0$

$$1 = \int \rho_\sigma(\varepsilon) \varepsilon (1 - \beta\varepsilon) \frac{d\varepsilon}{\sqrt{\xi^2(\varepsilon) + \Sigma_0^2 (1 - \beta\varepsilon)^2}}. \quad (14)$$

It defines the anisotropic superconducting order parameter of  $s^*$ -wave symmetry. The near-cylindrical hole-like  $\sigma$ -Fermi surfaces in MgB<sub>2</sub> gives room to calculate the superconducting DOS  $\rho(E) = \sum_p \delta(E - \sqrt{\varepsilon^2(p) + \Sigma^2(p)})$ , where the gap function is  $\Sigma = \Sigma_0(1 - \beta t(p)) = b(1 + a \cos^2 \vartheta)$ , where  $a = \beta w_1 / (12(1 - \beta w_1))$ ,  $b = \Sigma_0(1 - \beta w_1)$  and  $\vartheta$  is the azimuthal angle. Then the DOS normalized with respect to the normal DOS is

$$\frac{\rho(E)}{\rho_0(E)} = E \int_0^1 \frac{dz}{\sqrt{E^2 - b^2(1 + az^2)^2}}. \quad (15)$$

For a Coulomb repulsion such that  $\beta w_1 < 1$  the parameter satisfies  $a > 0$  and the

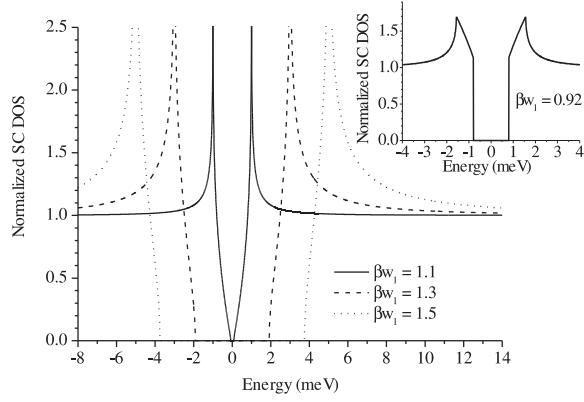


Figure 5: The superconducting DOS, normalized with respect to the normal DOS, for the Coulomb parameter range  $\beta w_1 > 1$ . At  $\beta w_1 = 0.92$ , the Maki result [16] is reproduced (inset).

superconducting DOS becomes

$$\begin{aligned} \frac{\rho(b < E < (1+a)b)}{\rho_0(E)} &= \sqrt{\frac{E}{2ab}} K(q), \\ \frac{\rho(E > (1+a)b)}{\rho_0(E)} &= \sqrt{\frac{E}{2ab}} F\left(\sin^{-1} \sqrt{\frac{ab}{(E+(1+a)b)q^2}}; q\right), \end{aligned} \quad (16)$$

which is expressed in terms of the complete and incomplete elliptic integrals  $K$  and  $F$ , respectively with modulus  $q = \sqrt{(E-b)/2E}$ .

The DOS (16) has cusps at  $E = \pm(1+a)b$ . A similar result was obtained in Ref. [15] for a non-specified parameter  $a > 0$ . In our case the parameter  $a$  is controlled by the in-plane Coulomb repulsion  $V$  as the authors of Ref. [20] noted. At  $\beta w_1 = 0.92$  the DOS of Eq. (16) (see Fig. 5, inset) reproduces Fig. 1(b) of Ref. [15].

For our case of an enhanced Coulomb repulsion  $\beta w_1 > 1$ , we have to take the parameter  $a < 0$  in the gap function and the superconducting DOS (Fig. 4) is then given by

$$\begin{aligned} \frac{\rho((1-|a|)b < E < b)}{\rho_0(E)} &= \frac{E}{\sqrt{(E+b)|a|b}} F\left(\sin^{-1} \frac{1}{q}; \sqrt{\frac{2E}{E+b}}\right), \\ \frac{\rho(E > b)}{\rho_0(E)} &= \sqrt{\frac{E}{2|a|b}} F\left(\sin^{-1} q; \sqrt{\frac{E+b}{2E}}\right). \end{aligned} \quad (17)$$

It contains two logarithmic divergencies at  $E = \pm b$  and a gap in the energy range  $|E| < (1-|a|)b$ . The two-gap ratio is  $1/(1-|a|)$ .

Measurements on  $\text{MgB}_2$  with scanning tunneling spectroscopy [24, 25] and with high-resolution photo-emission spectroscopy [26] revealed the presence of these two

gap sizes. From the ratio 3.3 between the two gaps in Ref. [24] we can extract the parameters  $|a| \approx 2/3$  and  $\beta w_1 \approx 1.14$ , whereas from data of Ref. [25] one can derive  $\beta w_1 = 1.21$ . A value  $\beta w_1 = 1.14$  can be estimated from Ref. [26]. Point-contact spectroscopy [27] shows gaps at 2.8 and 7 meV, from which we estimate a Coulomb repulsion parameter  $\beta w_1 = 1.16$ . The recent study of energy gaps in superconducting MgB<sub>2</sub> by specific-heat measurements revealed two gaps at 2.0 meV and 7.3 meV [28] for which  $\beta w_1 = 1.13$ , and a gap ratio 3 – 2.2 [29], for which  $\beta w_1 = 1.14$ –1.15. Measurements of the specific heat of Mg<sup>11</sup>B<sub>2</sub> also give evidence for a second energy gap [30]. Raman measurements [31] established pronounced peaks, corresponding with gaps at 100 cm<sup>-1</sup> and 44 cm<sup>-1</sup>. From these data one can extract  $a = -0.56$  and  $\beta w_1 = 1.18$ . At  $\beta w_1 = 1$  we have gapless like superconductivity. In this case the superconducting DOS is linear with respect to the energy near the nodes of the superconducting order parameter. Then the superconducting specific heat  $C_e \sim T^2$  and the NMR boron relaxation rate  $\sim T^3$  at low temperatures. From this point of view it is interesting that the data of Ref. [32] shows a  $C_e \sim T^2$  behaviour and a deviation from the exponential BCS behaviour in  $T_1^{-1}(T)$  of <sup>11</sup>B [33] visualized in MgB<sub>2</sub>.

### 3 Conclusions

We have done a GL analysis of the superconductivity of a two-band superconductor with particular attention to MgB<sub>2</sub>. In that framework, we provide the different possibilities for a T-P phase diagram, make predictions for the role of the bands and discuss different experiments from which crucial information can be extracted. Then we have analyzed the superconducting properties of the material MgB<sub>2</sub> within the framework of a correlated model Eq. (7). The existing electron-phonon and non-phonon approaches to the superconducting mechanism in MgB<sub>2</sub> can be separated in two groups: one pays attention to the  $\sigma$ -electrons and the other to the  $\pi$ -electron subsystem. We have taken into account both the correlated  $\sigma$ - and noncorrelated  $\pi$ -electrons. Analysis of our results leads to the conclusion that superconductivity occurs in the subsystem of  $\sigma$ -electrons with degenerate narrow energy bands whereas the wide-band  $\pi$ -electrons play the role of a reservoir. Superconductivity is driven by a non-phonon kinematic interaction in the  $\sigma$ -band. A lot of evidences in favour of two different superconducting gaps can be explained by anisotropic superconductivity with an order parameter of  $s^*$ -wave symmetry, induced by the in-plane Coulomb repulsion. For an enhanced interboron Coulomb repulsion ( $\beta w_1 > 1$ ) the logarithmic divergencies in the superconducting DOS (Eq. 17, Fig. 5) are manifested by a second gap in the experiments. In our approach the electron-phonon coupling is hidden in the parameter  $r$ . Therefore the pressure and isotope effects can be explained by the dependence of  $r(\omega)$  on the phonon modes. From the non-monotonic  $T_c$  dependence on  $r$  it follows that the MgB<sub>2</sub> material is in the underdoped regime (around  $r \gtrsim$

$-w_1/4$ ). For a fictitious system  $A^{2+}B_2$ , where the two electrons are contributed by atom A, the superconducting critical temperature increases with an  $r$  increase. A pressure increase lowers the  $\sigma$ -band with an  $r$  decrease resulting in a negative pressure derivative of  $T_c$  in agreement with experiment [34]. The bell shaped curve  $T_c(r)$ , with the  $MgB_2$  position in the underdoped regime, shows a possibility to reach higher  $T_c$ 's in diboride materials with an  $AlB_2$  crystal structure. We suggest the synthesis of materials with increased  $r$ -values (e.g. with "negative chemical pressure") and optimized smaller interatomic B-B distances in the honeycomb plane.

## Acknowledgments

This work was supported by the Flemish Science Foundation (FWO-VI), the Concerted Action program (GOA), the Inter-University Attraction Poles research program (IUAP-IV) and the University of Antwerp (UOA).

## References

- [1] J. Nagamatsu *et al.*, Nature **410**, 63 (2001).
- [2] J. J. Betouras, V. A. Ivanov and F. M. Peeters, submitted to Phys. Rev. Lett.
- [3] D. F. Agterberg, E. Demler, and B. Janko, cond-mat/0201376.
- [4] A. F. Goncharov *et al.*, cond-mat/0104042; Phys. Rev. B **64**, 100509(R) (2001).
- [5] V. G. Tissen *et al.*, cond-mat/0105475.
- [6] T. Vogt *et al.*, Phys. Rev. B **63**, 220505(R) (2001).
- [7] M. Ozaki, Prog. Theor. Phys. **75**, 442 (1986); M. Sigrist, R. Joynt, and T. M. Rice, Phys. Rev. B **36**, 5186 (1987).
- [8] M. Sigrist and K. Ueda, Rev. Mod. Phys. **63**, 239 (1991)
- [9] J. M. An and W. E. Pickett, Phys. Rev. Lett. **86**, 4366 (2001).
- [10] C. Panagopoulos *et al.*, Phys. Rev. B **64**, 4514 (2001)
- [11] J. Betouras and R. Joynt, Europhys. Lett., **31**, 119 (1995); J. J. Betouras and R. Joynt, Phys. Rev. B **57**, 11752 (1998)
- [12] R. Joynt, Phys. Rev. Lett. **71**, 3015 (1993)
- [13] T. Yildirim *et al.*, Phys. Rev. Lett. **87**, 037001 (2001).

- [14] J. S. Schilling *et al.*, to appear in: *Studies of High-Temperature Superconductors* (ed. A. Narlikar), Vol. 38, (Nova Science, NY,2002); cond-mat/0110268.
- [15] S. Haas and K. Maki, Phys. Rev. B **65**, 020502 (2002).
- [16] I. M. Lifshits, Sov. Phys. JETP **11**, 1130 (1960).
- [17] M. Monteverde *et al.*, Science **292**, 75 (2001).
- [18] D. R. Armstrong, P. G. Perkins, J. Chem. Soc. Faraday II 75, 12 (1979).
- [19] N. I. Medvedeva *et al.*, JETP Lett. 73, 336 (2001)
- [20] K. Voelker, V. I. Anisimov, T. M. Rice, cond-mat/0103082.
- [21] Y. Kong *et al.*, Phys. Rev. B 64, R020501 (2001).
- [22] V. A. Ivanov, M. van den Broek and F. M. Peeters, Solid State Commun. **120**, 53 (2001).
- [23] V. Ivanov, Europhys. Lett. 52, 351 (2000).
- [24] C.-T. Chen *et al.*, cond-mat/0104285.
- [25] F. Giubileo *et al.*, cond-mat/0105592.
- [26] S. Tsuda *et al.*, cond-mat/0104489.
- [27] P. Szabo *et al.*, cond-mat/0105598.
- [28] R. A. Fisher *et al.*, cond-mat/0107072.
- [29] A. Junod *et al.*, to appear in: *Studies of High-Temperature Superconductors* (ed. A. Narlikar), Vol. 38, (Nova Science, NY,2002); cond-mat/01106394.
- [30] F. Bouquet *et al.*, Phys. Rev. Lett. 87, 047001 (2001)
- [31] X. K. Chen *et al.*, cond-mat/0104005 version 2 (21 May 2001)
- [32] Y. Wang, T. Plackowski, A. Junod, Physica C 355, 179 (2001).
- [33] A. Gerashenko *et al.*, cond-mat/0102421.
- [34] H. Tou *et al.*, J. Phys.: Condens. Matter 13, L267 (2001).